Studies on the Formation and Physical Chemical Properties of Synthetic Myosin Filaments*

Robert Josephs† and William F. Harrington

ABSTRACT: The properties of myosin filaments formed by dialysis of solutions of monomeric myosin (in 0.5 M KCl) against 0.1–0.3 M KCl in the pH range 6.2–8.5 have been investigated. In the pH range 6.2–7.3 three heterogeneous weight classes of filaments are observed which have infinite dilution sedimentation coefficients ($s^0_{20,w}$) of 1100, 330, and 180 S. Electron microscope studies indicate that the 1100S particles are 2–12 μ long, and the lengths of the 180S particles lie in the range 0.4–3.0 μ, and bear many topological similarities to the synthetic myosin polymers described by Huxley. In the pH range 8–8.5, a single hypersharp polymer peak was observed with $s^0_{20,w}$ = 150 S. A length-distribution histogram obtained from electron microscope measurements indicates that about 70% of the particle lengths lies between 5600 and 7500 A with a mean length of all particles near 6300 A. The molecular dimensions of the 150S particle evaluated from the shear dependence of the intrinsic viscosity, velocity sedimentation, and electron microscopic data yielded a molecular weight of 50–60 $\times$ 10^6, a length of about 6500 A, a particle diameter of 120 A, and an axial ratio between 50 and 60. Evidence is presented supporting the view that the myosin monomer is in equilibrium with the polymer, and that the equilibrium can be described in terms of a simple mass action expression.

The position of the monomer $\rightleftharpoons$ polymer equilibrium is sensitive to salt concentration, pH, and the hydrostatic pressure. The relationship between the structure of the synthetic filaments and the native thick filament of the myofibril is considered.

Although myosin exists as essentially monodisperse protein molecules in aqueous solutions of high ionic strength (0.5 M KCl), the work of several investigators (Jakus and Hall, 1947; Noda and Ebashi, 1960; Huxley, 1963; Zobel and Carlson, 1963) has demonstrated that at intermediate ionic strengths (0.1–0.3 M) the myosin monomers associate to form systems of polydisperse filament-like polymers. The lengths of the filaments generated in the ionic strength range 0.02–0.3 M (pH 5.9–7.4) have been investigated by flow birefringence (Noda and Ebashi, 1960) and the results indicate the presence of particles of lengths varying between 7000 and 20,000 A depending on the ionic strength and pH. Moreover the polymers can be readily and completely dissociated into the monomeric units by increasing the salt concentration.

Additional information on the physical properties and fine structure of these filaments has come from the electron microscope studies of Huxley (1963) who has reported that a system of filaments heterogeneous in length is formed at an ionic strength of 0.15 M which shows several morphological features in common with the native thick filaments of the myofibril. These features include a diameter of about 125 A and a smooth central region of the order of 1500–2000 A. On either side of the bare central region irregular projections appear to cover the surface of the filaments out to the ends which have a tapered appearance very similar to that of the thick filaments observed in electron micrographs of thin longitudinal sections of muscle (Huxley, 1960).

Kaminer and Bell (1966) have recently reported that shorter particles of more uniform length are generated at high pH (8.0) and at low ionic strength (0.10). The length of the myosin filaments thus prepared ranges between 2000 and 5000 A with a mean value of 4000 A. An ultracentrifuge experiment yielded a hypersharp peak having a sedimentation coefficient of 21 S (c = 0.24%) and a small amount of slowly sedimenting material which the authors suggest may be monomeric myosin.

In the work to be presented below, we have investigated the solution properties of myosin filaments formed by dialysis of monomer solutions (in 0.5 M KCl) against solutions of ionic strengths between 0.1 and 0.3 M KCl and pH values spanning the range 6.2–8.5. The assembled information collected from both hydrodynamic and electron microscope studies indicates that, although the size of the myosin polymers is critically dependent upon the ionic environment pre-

* From the Department of Biology, McCollum-Pratt Institute, Johns Hopkins University, Baltimore, Maryland. *Received July 18, 1966.* Contribution No. 47[9], McCollum-Pratt Institute. This investigation was supported by U. S. Public Health Service Grant AM-04349. One of us (R. J.) acknowledges a predoctoral fellowship from the U. S. Public Health Service. This work was presented in part at the Symposium on Biological Movement, Toranomon, Tokyo, Sept 14–17, 1965.

† The material presented here was taken in part from a thesis submitted to the Graduate School of the Johns Hopkins University in partial fulfillment of the requirements for the degree of Doctor of Philosophy.

vailing during their formation, nevertheless particles of all sizes appear to share a common structural pattern. In the pH range between 6.2 and 7.3, three weight classes of polymers were observed in the ultracentrifuge. Each of these was heterogeneous with respect to size and hence not readily amenable to meaningful physical characterization. Under most conditions studied, significant amounts of monomer are also present, further complicating the interpretation of the hydrodynamic data. Thus the sedimentation and electron microscope studies carried out on these preparations give a qualitative rather than a quantitative description of their properties. On the other hand a single polymer species of relatively narrow size distribution is observed in equilibrium with monomeric myosin over the range pH 8.0–8.5, and this system was extensively characterized by conventional hydrodynamic methods. These latter preparations of reconstituted myosin filaments represent a new type of experimental material, the study of which may yield quantitative information pertinent to an understanding of the equilibrium between the myosin monomer and polymer as well as the magnitude of the forces responsible for causing the association of the monomer into the highly differentiated, complex macrostructure of the native thick filament.

Materials and Methods

Reagents. Distilled water and analytical grade reagents were used in all experiments.

Preparation of Myosin. Myosin was prepared from rabbit muscle as previously described (Kielley and Bradley, 1956).

Preparation of Solutions of Myosin Polymers. Solutions of myosin polymers were prepared by dialysis of monomeric myosin (in 0.5 M KCl) against two changes of 100 volumes of KCl solution of the desired ionic strength and pH for at least 24 hr. Solutions were stirred continuously during dialysis. Dilution of the protein solution to the appropriate concentration range was always performed *prior* to dialysis. In the pH range between 6.2 and 7.3 phosphate buffer was used, and for the pH range 8.0–8.5 Veronal buffer was used. In all cases the buffer concentration was 2×10^{-3} M. A few experiments were made at pH 8.0 using phosphate buffer, but no differences were observed between the sedimentation profiles or sedimentation coefficients of polymers thus prepared and those dialyzed against Veronal buffer. Dialysis tubing, size 8/100 (Union Carbide), was prepared for use by soaking in a hot (80°) sodium bicarbonate solution (1 M) for 10–15 min, followed by copious washing with distilled water. Polymer solutions were clarified following completion of dialysis by spinning at 7000*g* for 1 or 2 min.

Protein Concentration. The total protein concentration of the polymer solutions was determined spectrophotometrically using the extinction coefficient previously reported for monomeric myosin (ϵ_{279} 543 cm²/g; Kielley and Harrington, 1960). Because of the high level of light scattered by the polymer solutions, depolymerization is mandatory prior to spectrophotometric determination of concentration. Depolymerization was achieved by making gravimetric dilutions with concentrated KCl solutions (final concentration of KCl was 0.4–0.7 M). In a number of experiments the protein concentration was also determined utilizing the Rayleigh interference optical system of the ultracentrifuge and a 30-mm synthetic boundary cell. The concentrations obtained using interference optics agreed within experimental error with those obtained spectrophotometrically.

Viscosity. The viscosities of polymer solutions were measured in Ostwald-type glass capillary viscometers as a function of both shearing stress (τ) and concentration. Two different viscometers were used in this study: (1) a three-bulb, Ostwald-type viscometer with shearing stresses of 3.00, 1.73, and 0.51 dynes/cm²; (2) a single-bulb, Ostwald-type viscometer having a shearing stress of 2.39 dynes/cm². Calibration of the viscometers and treatment of the non-Newtonian viscosity data followed the procedures described by Yang (1961). Corrections for inhomogeneous flow in the capillary viscometers were applied.

Electron Microscopy. All samples were examined in an RCA-EMU-3 electron microscope using a 37.5-μ Pt objective aperture, with an accelerating voltage of 50 kv. Calibration of the magnification was performed by the use of standard polystyrene spheres. The diameter of these particles specified by the supplier (Dow Chemical Co.), 1880 ± 80 A, was confirmed by dissymmetry measurements using a Brice-Phoenix Model 1000D light-scattering photometer. The diameter of the spheres on enlarged prints was measured with an ocular rule having calibrations of 0.1 mm, and the lengths of the particles were measured with a ruler. All fields used for determining particle dimensions contained several spheres.

Negatively stained samples were prepared in the manner previously described by Huxley (1963), except that a low concentration of negative stain (0.2–0.4% uranyl acetate) was used in an attempt to minimize degradation of the myosin polymers. Although this procedure yielded preparations which were predominantly positively stained, small areas on the grid were found to be negatively stained. Grids prepared in this manner were suitable for length determinations, but were inadequate for fine structure analysis except in the negatively stained regions.

Ultracentrifugation. Ultracentrifugation experiments were carried out at rotor temperatures close to 5° utilizing a Spinco Model E ultracentrifuge equipped with a phase plate and an RTIC unit. Either single-sector Kel-F centerpieces or double-sector epon centerpieces were used. The epon centerpieces were coated with Krylon (an acrylic resin manufactured by Krylon, Inc., Norristown, Pa.) to prevent interaction of the polymer solutions with the aluminum filler of the epon. When polymer solutions having concentrations below 0.15 g/100 ml were studied, centerpieces with a light path length of 30 mm were used instead of the

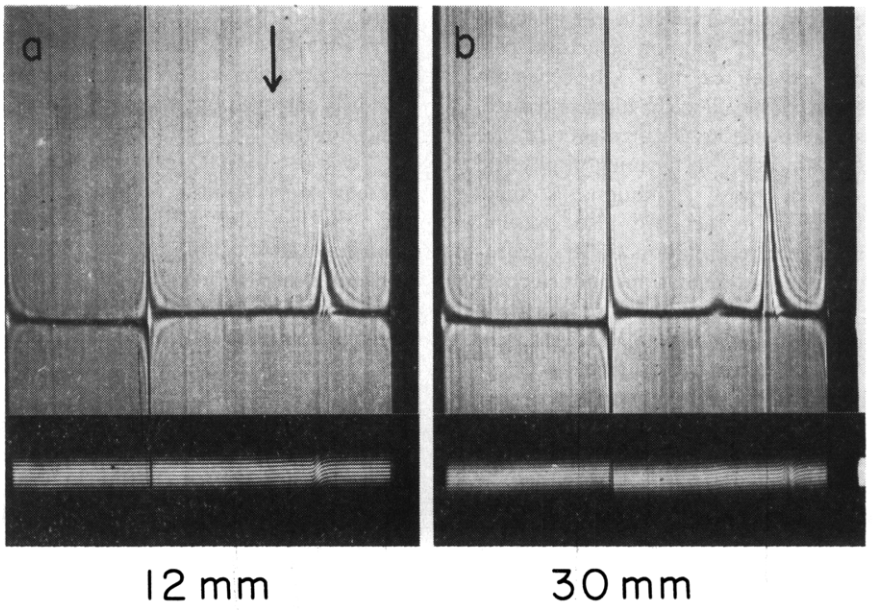

FIGURE 1: Comparison of sedimentation profiles of myosin polymers (pH 8.3, 0.137 M KCl) observed using 12- and 30-mm synthetic-boundary cells. The arrow in a indicates the position at which the synthetic boundary was formed. Protein concentration 0.084%, 13,410 rpm for both a and b. Bar angle is 60°.

usual 12-mm centerpieces. Thus very small amounts of monomer present in polymer solutions could be readily measured with the aid of a 30-mm double-sector, synthetic-boundary interference cell, whereas measurement would have been virtually impossible with the conventional 12-mm synthetic-boundary cell (Figure 1).

Velocity sedimentation studies were performed with both single-sector and double-sector cells at rotor velocities of 10–20 $\times$ 10^3 rpm, and the calculated sedimentation coefficients were corrected to a standard state of water at 20°. It was necessary to use low speeds for velocity experiments, since high rotor speeds cause shifts in monomer–polymer equilibrium (see below). Concentrations of monomer and polymer in the pH 8.3 equilibrium system were estimated either from schlieren peak areas or from the fringe count and were corrected for radial dilution.

Results

When myosin solutions in 0.5 M KCl are dialyzed against low ionic strength buffers and the resulting solutions examined in the ultracentrifuge at low temperature, schlieren patterns show the presence of discrete, high molecular weight sedimenting components. The number of these rapidly sedimenting peaks and their gross appearance depends on the ionic strength and pH of the buffer. In general the peaks are asymmetric, exhibiting a high degree of self-sharpening on the solvent side, trailing off on the solution side of the boundary as expected for relatively polydisperse, highly elongated particles.

In the present study an attempt was made to find ionic conditions which would yield a relatively monodisperse myosin polymer. For this reason a wide range of pH and ionic strength conditions were systematically examined. It was found that over the range pH 6.2–7.8 at all ionic strengths (0.09–0.3) a multicomponent polymer system was present, whereas at pH values between pH 8.0 and 8.5 only a single hypersharp polymer boundary was observed. The sedimentation behavior of the polymeric species was examined at low rotor velocities (15,000–30,000 rpm), and then the rotor velocity of the centrifuge was increased to 60,000 rpm to determine the amount and sedimentation coefficient of the lower molecular weight myosin monomer remaining in solution.

Studies on the Multicomponent Polymer System in the Range pH 6.2–7.2

Only three distinctive types of sedimentation patterns were observed in this pH range at all ionic strengths which were examined:

(I) A single asymmetric rapidly sedimenting boundary with infinite dilution sedimentation coefficient $s^0_{20,w}$ = 1100 S with virtually no myosin monomer present; this type of system was observed at ionic strengths below 0.2 M KCl over the entire pH range 6.2–7.3. (Figure 2).

(II) A two-peak system with infinite dilution sedimentation coefficients $s^0_{20,w}$ = 1100 S and $s^0_{20,w}$ = 330 S; this type of sedimentation pattern was observed at intermediate ionic strengths in the neighborhood of 0.3 M KCl and over the pH range 6.2–6.6. The amount of myosin monomer present at any given total protein concentration was greater than in I (Figure 3).

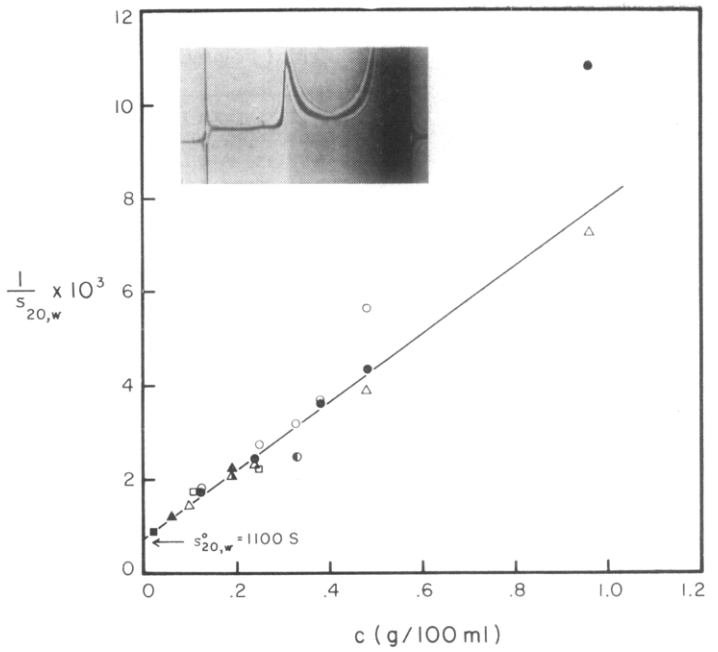

FIGURE 2: Reciprocal of the sedimentation coefficient ($1/s_{20,w}$) *vs.* concentration for the type I polymer system. ▲, pH 6.2, 0.20 M KCl; ◐, pH 7.1, 0.10 M KCl; ○, pH 7.1, 0.20 M KCl; ●, pH 6.8, 0.25 M KCl; ◭, pH 6.8, 0.20 M KCl; □, pH 7.0, 0.12 M KCl; △, pH 7.1, 0.1 M KCl, 4×10^{-3} M ATP, 2×10^{-3} M $MgCl_2$, 10^{-3} M EDTA, 4×10^{-3} M phosphate; ■, pH 6.4, 0.1 M KCl. Insert: typical sedimentation profile of type I polymer system at 17,980 rpm. Protein concentration is 0.32%, pH 7.1, 0.10 M KCl. Bar angle is 60°.

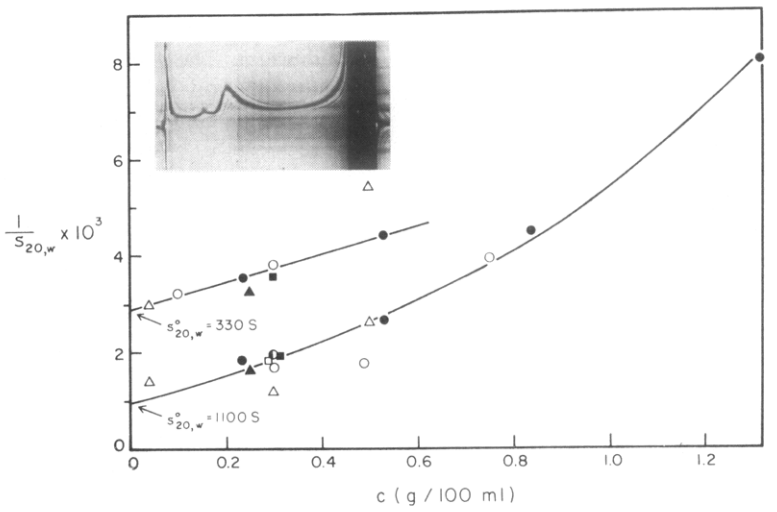

FIGURE 3: Reciprocal of the sedimentation coefficient ($1/s_{20,w}$) *vs.* concentration for the type II polymer system. ●, pH 6.3, 0.325 M KCl; ○, pH 6.7, 0.30 M KCl; △, pH 6.2, 0.30 M KCl; ◐, pH 6.7, 0.27 M KCl; □, pH 6.8, 0.26 M KCl; ■, pH 6.95, 0.23 M KCl; ▲, pH 7.3, 0.20 M KCl. Insert: typical sedimentation profile of type II polymer system run at 15,220 rpm. Protein concentration is 0.53% (note partial boundary of monomer at meniscus trace), pH 6.3, 0.325 M KCl. Bar angle is 60°.

(III) A two-peak system with infinite dilution sedimentation coefficients $s^0_{20,w}$ = 330 S and $s^0_{20,w}$ = 180 S, this type of sedimentation pattern was observed in the region of 0.30 M KCl but at higher pH values (pH 6.8–7.1). The amount of monomer present at any given total protein concentration was greater than in II (Figure 4). At ionic strengths higher than 0.35 M only a single boundary with sedimentation coefficient characteristic of the myosin monomer (~6 S) was detected at all pH values.

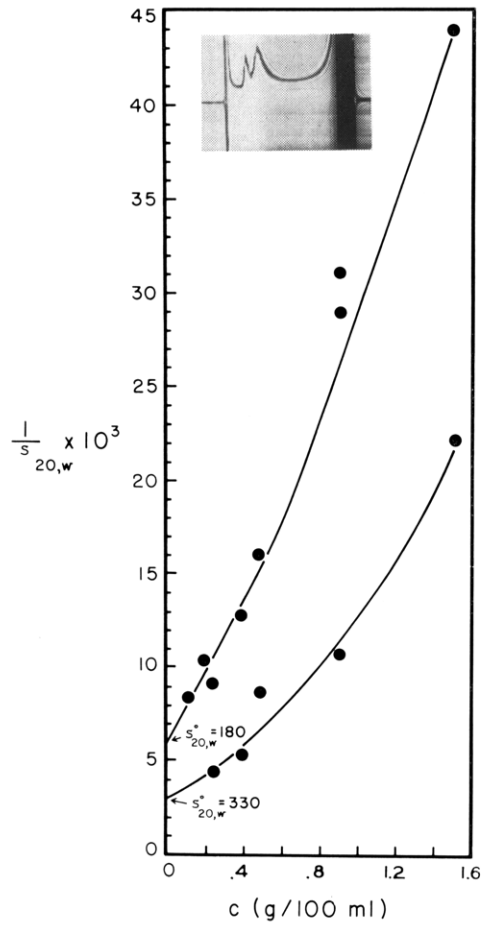

FIGURE 4: Reciprocal of the sedimentation coefficient ($1/s_{20,w}$) *vs.* concentration for the type III polymer system. pH 6.8, 0.30 M KCl. Insert: typical sedimentation profile of type III polymer system run at 21,740 rpm. Protein concentration is 0.48%. Bar angle is 60° (note partial boundry of monomer at meniscus trace).

Table I summarizes the ionic conditions required for formation of each type of polymer system. To establish the identity of a given polymer species as well as the system class, the reciprocal of the measured sedimentation coefficients obtained at various protein concentrations were plotted against total protein concentration for each system and the resulting curves extrapolated to infinite dilution.

The reciprocals of the sedimentation coefficients *vs.* total protein concentration for the single polymer boundary observed in the various solvents generating the type I centrifuge patterns are given in Figure 2. Although the data show an appreciable amount of scatter, all of the points fall about a single smooth curve with infinite dilution value of $s^0_{20,w}$ = 1100 S.

Plots of the reciprocal of the sedimentation coefficient *vs.* total protein concentration for the two polymer boundaries observed in the type II centrifuge patterns are given in Figure 3. On dilution of the protein concentration for the type II systems, the relative ratio of the monomer:polymer peak area is increased, suggesting that these systems are in monomer–polymer equilibrium. The major peak of this system has an infinite dilution value of about 1100 S. In addition to this component a significant amount of monomer ($s^0_{20,w}$ = 6 S) is always present as well as a small amount of a component with infinite dilution value of 330 S. Comparison of the $1/s_{20,w}$ *vs.* *c* plots of the 1100S polymer in Figure 2 and Figure 3 reveals that the slope of the plot is much lower in the two-peak system. We believe that this results from the fact that the "true" concentration of this component in solution is lower than the total protein concentration plotted, leading to a higher value of the sedimentation coefficient at any particular protein concentration.

The major high molecular weight peak observed in the type III centrifuge patterns exhibits an infinite dilution sedimentation coefficient of 330 S. This component is accompanied by a slower sedimenting polymer present in lower concentration with $s^0_{20,w}$ = 180 S. Over 40% of the total mass of myosin was present as monomer in these ultracentrifuge experiments, the amount depending on the total protein concentration. Relative ratios of the peak areas of the sedimenting components in type III systems were found to be much more sensitive to small changes in the salt concentration than the type I and II systems, leading to considerable difficulty in reproducibility. Dilution of the protein favored formation of the monomer and the slower sedimenting (180 S) polymer species. In Figure 4 the reciprocal of the sedimentation coefficients observed

TABLE I: Ionic Conditions Used in Formation of Different Polymer Classes.

pH	KCl	Class[a]	pH	KCl	Class[a]
6.2	0.2	I	6.66	0.30	II
6.4	0.1	I	6.8	0.26	II
6.8	0.2	I	6.95	0.23	II
6.8	0.25	I	7.3	0.20	II
7.1	0.1[b]	I	7.1	0.25	III
7.0	0.12	I	6.8	0.3	III
7.0	0.2	I	6.3	0.4	Monomer
6.2	0.3	II	6.8	0.35	Monomer
6.3	0.325	II	7.1	0.3	Monomer
6.66	0.27	II			

[a] Class I: one polymer peak, little or no monomer, $s^0_{20,w}$ = 1100 S (see Figure 2). Class II: two polym r peaks, 10–60% monomer; depending on protein concentration $s^0_{20,w}$ = 1100 and 330 S (see Figure 3). Class III: two polymer peaks, 40–90% monomer; depending on protein concentration $s^0_{20,w}$ = 330 and 180 S (see Figure 4). [b] Plus relaxing medium (10^{-3} EDTA, 2×10^{-3} $MgCl_2$, 4×10^{-3} adenosine triphosphate, and 4×10^{-3} PO_4).

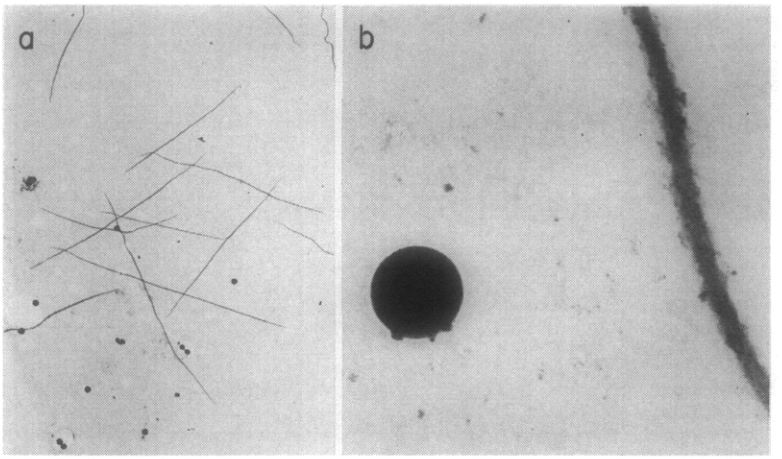

FIGURE 5: Type II myosin polymer filaments prepared by dialysis of monomeric myosin (in 0.5 M KCl) against pH 6.2, 0.30 M KCl. See Figure 6 for the length distribution. The polystyrene spheres are 1880 A in diameter.

in the type III centrifuge patterns are plotted against total protein concentrations.

In summary, the amount and relative distribution of the three high molecular weight polymer species depend on both the ionic strength and pH. As the pH and ionic strength are raised, the 330S and 180S particles are favored and, under these conditions, an increasing amount of more slowly sedimenting material is observed with sedimentation coefficient characteristic of monomeric myosin.

Electron Microscopy of Myosin Polymers in the Range pH 6.2–7.3

Stained Preparations. Additional information on the structure of the myosin polymers and their size distribution was obtained from electron microscopy. Only type II (pH 6.2, 0.3 M KCl) and type III (pH 7.1, 0.25 M KCl) systems were examined.

Observations on the Type II System. A polymeric type II myosin system was diluted to a concentration of 0.06% with dialysate containing 0.5% formaldehyde, applied to a formvar covered microscope grid, and stained. At low magnification (Figure 5), electron micrographs show a system of threadlike particles polydisperse in both length and diameter. The lengths vary from 2 to 12 μ with a large fraction lying between 6.5 and 9.5 μ. Frequently the ends of the filament appear to be so closely intertwined that they give the appearance of a single, continuous thread. A histogram of the particle lengths (Figure 6) emphasizes the polydispersity of the type II system indicated earlier in the ultracentrifuge studies and demonstrates that most of the particles are longer than 5 μ, a finding consistent with the high sedimentation value (1100 S) of the most rapidly sedimenting species. Examination of a number of fields obtained at high magnification (Figure 5) reveals that the surface of the particles is not smooth but rather appears to have irregular protuberances. The diameters of the filaments lie between 300 and 500 A.

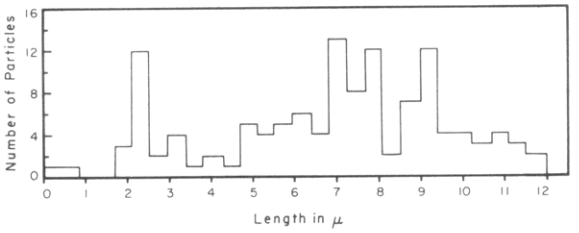

FIGURE 6: Histogram of length distribution for 120 particles of the type II polymer system.

Observations on the Type III System. Figure 7 presents a low magnification photograph of a type III polymeric system. The lengths of 163 particles are plotted in the histogram presented in Figure 8 showing a relatively narrow distribution (from about 0.4 to 3.0 μ) with a mean particle length of 1.2 μ. In general these particles exhibited structural features similar to those observed and described by Huxley (1963) in his electron microscope studies of synthetic myosin filaments. As noted above, sedimentation studies of the type III system showed that reduction of the protein concentration favored the dissociation of the high molecular weight rapidly sedimenting polymeric species into the more slowly sedimenting polymer species. Thus, in view of the low concentrations of protein used for the electron microscope studies it seems possible that the particles observed may represent primarily the slower sedimenting 180S component. In this connection it should be noted that when low concentrations of protein were examined in the type III system (less than 0.18%) only the 180S polymer was detected in the schlieren patterns.

Studies of Myosin Polymers Formed in the Range pH 8.0–8.5

The complex sedimentation patterns observed upon ultracentrifugation of myosin solutions over the pH

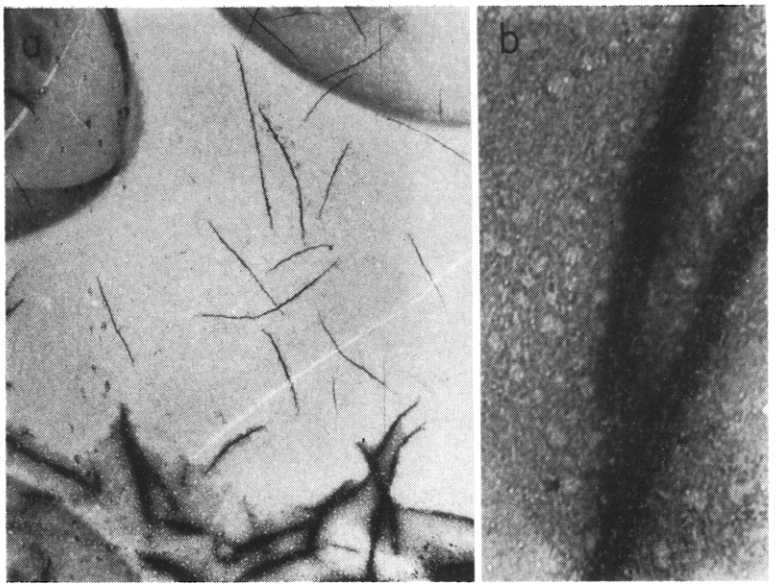

FIGURE 7: Type III myosin polymer filaments prepared by dialysis of monomeric myosin (in 0.5 M KCl) against pH 7.1, 0.25 M KCl. See Figure 8 for the length distribution.

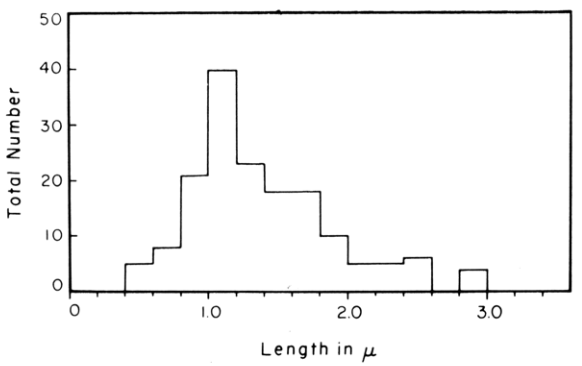

FIGURE 8: Histogram of length distribution for 163 particles of the type III polymer system.

range 6.2–7.3 are not seen above pH 8. As the pH is raised the multipeak schlieren pattern is transformed into a system consisting of a single hypersharp polymer boundary. Monomer is always present under these conditions, and as in the studies at lower pH, its relative magnitude depends upon the ionic environment and the total protein concentration. The effect of pH on the area of the polymer boundary at a constant ionic strength (0.15 M KCl) and protein concentration (0.13%) is presented in Figure 9. Even at this low protein concentration it will be seen that the polymer boundary maintains its integrity. The proportion of monomer present increases with increasing pH as can be seen from the increasing area of the monomer boundary as well as in the reduction in area of the polymer boundary.

The complementary experiment of maintaining constant pH and varying the ionic strength gives the ultracentrifuge patterns shown in Figure 10. This experiment demonstrates that an increase in salt concentration leads to a striking depletion in the polymer boundary and a consequent buildup in the amount of monomer as judged from the boundary at the meniscus. The redistribution of mass occurs over a relatively narrow range of salt concentration (μ = 0.12–0.22 M) and emphasizes the important role played by the salt in maintaining the delicate balance between the two species.

In view of the remarkably sharp polymer boundaries obtained under the ionic conditions described above, we were encouraged to investigate the effects of incremental changes in both pH and ionic strength in this region to establish optimum conditions for the preparation of a homogeneous myosin polymer. Dialysis of myosin solutions against two changes of pH 8.3, 0.137 M KCl buffer yielded a system exhibiting a hypersharp boundary comparable in appearance to that of tobacco mosaic virus and with a minimal amount of monomer as judged from the schlieren patterns (see Figure 11). A single polymer boundary was observed over the concentration range examined (0.02–0.8%).

Although monomer is present at very low concentrations under the conditions described above and in fact is not readily detected in a conventional run, its presence can nevertheless be confirmed by a synthetic-boundary experiment utilizing a 30-mm path-length cell (see Figure 1). Using the Rayleigh optical system in conjunction with a 30-mm path-length cell it was determined that the amount of monomer remained virtually constant at about 1.0 fringe (0.01%) when the total protein concentration varied from 0.085 to 0.027%. This behavior is consistent with that expected for a

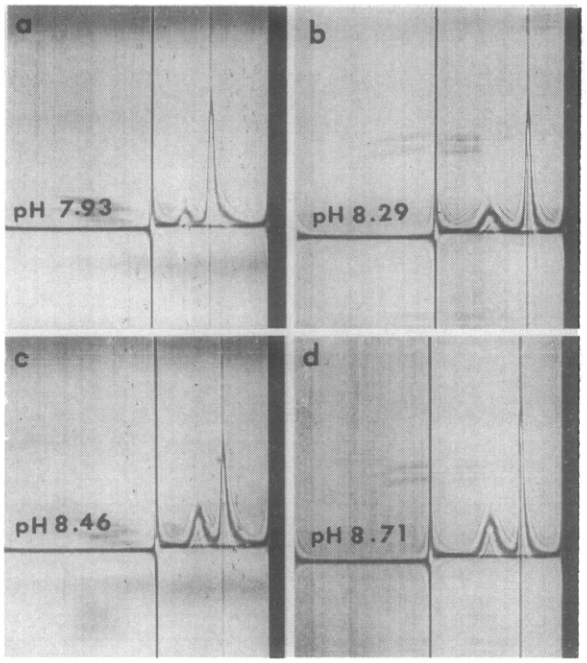

FIGURE 9: The effect of pH on the monomer–polymer equilibrium. All experiments were carried out in 0.15 M KCl, at the indicated pH in 30-mm double-sector capillary-type synthetic-boundary cells, at 11,000 rpm with a bar angle of 60° and a total protein concentration of 0.13%.

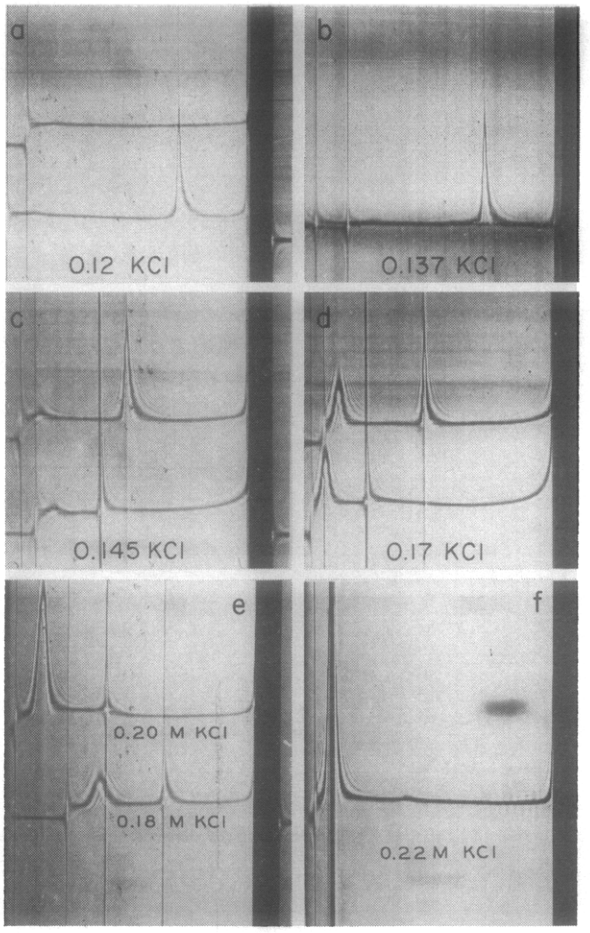

FIGURE 10: Effect of ionic strength on the monomer–polymer equilibrium at pH 8.3. Bar angle is 60°; 12-mm light path. (a) Lower pattern, protein concentration 0.25%; 27,690 rpm; upper pattern, solvent. (b) Protein concentration 0.21%; 19,160 rpm. (c) Protein concentration, lower pattern 0.51%; upper (wedge window) pattern 0.27%, 29,500 rpm. (d) Protein concentration, lower pattern 0.7%; upper (wedge window) pattern 0.34%, 29,500 rpm. (e) Protein concentration 0.7% in both cells, 24,630 rpm. (f) Protein concentration 0.7%, 24,630 rpm.

monomer $\rightleftharpoons$ polymer equilibrium obeying the conditions described by Gilbert (1955, 1958, 1959) and Gilbert and Gilbert (1962) (also see Nichol *et al.*, 1964). Although an increase in salt concentration to 0.17 M KCl displaces the monomer $\rightleftharpoons$ polymer equilibrium in favor of the monomer, the $1/s$ *vs.* c plot of the polymer, when corrected for the concentration of monomer, is unchanged. Under these ionic conditions a significant fraction of the protein was present as monomer at all concentrations examined (see Figures 10 and 12) and the area of the monomer boundary in schlieren photographs showed little change (from 0.08 to 0.07%) over a relatively large change in total protein concentration (0.84–0.10%), respectively (Figure 13).

A plot of the reciprocal of the sedimentation coefficient of the polymer boundary against total protein concentration is presented in Figure 14. We attribute the appreciable scatter in the experimentally determined sedimentation coefficients apparent in Figure 14 to both the extreme $1/s$ *vs.* c dependence of the asymmetric polymer particles and the high sensitivity of the monomer $\rightleftharpoons$ polymer equilibrium to small variations in the salt concentration. A least-squares analysis of all of the data giving equal weight to each point yields an infinite dilution value of $s^0_{20,w} = 150$ S.

As we have indicated below, at pH 8.3 and 0.17 M KCl both the myosin monomer and the 150S polymer are observed simultaneously in the ultracentrifuge (Figures 10d and 12a). When the centrifuge is operated at low speed (15,000–30,000 rpm) the polymer moves through the cell as a hypersharp peak and the base line between monomer and polymer appears flat. If, during the run, the rotor velocity is quickly increased to 60,000 rpm a new boundary emerges on the slow side of the polymer boundary, *i.e.*, it is "uncovered" by the polymer boundary. One then sees three peaks in the schlieren optical system (Figure 12b). The peak nearest the meniscus has the sedimentation coefficient of myosin (5.4 S); the newly formed peak has a *slower* sedimentation coefficient (4.4 S) than myosin, and the polymer boundary retains its characteristic sedimentation coefficient, but the area under this peak is continuously depleted as it migrates radially. The newly formed peak exhibits the characteristics of a

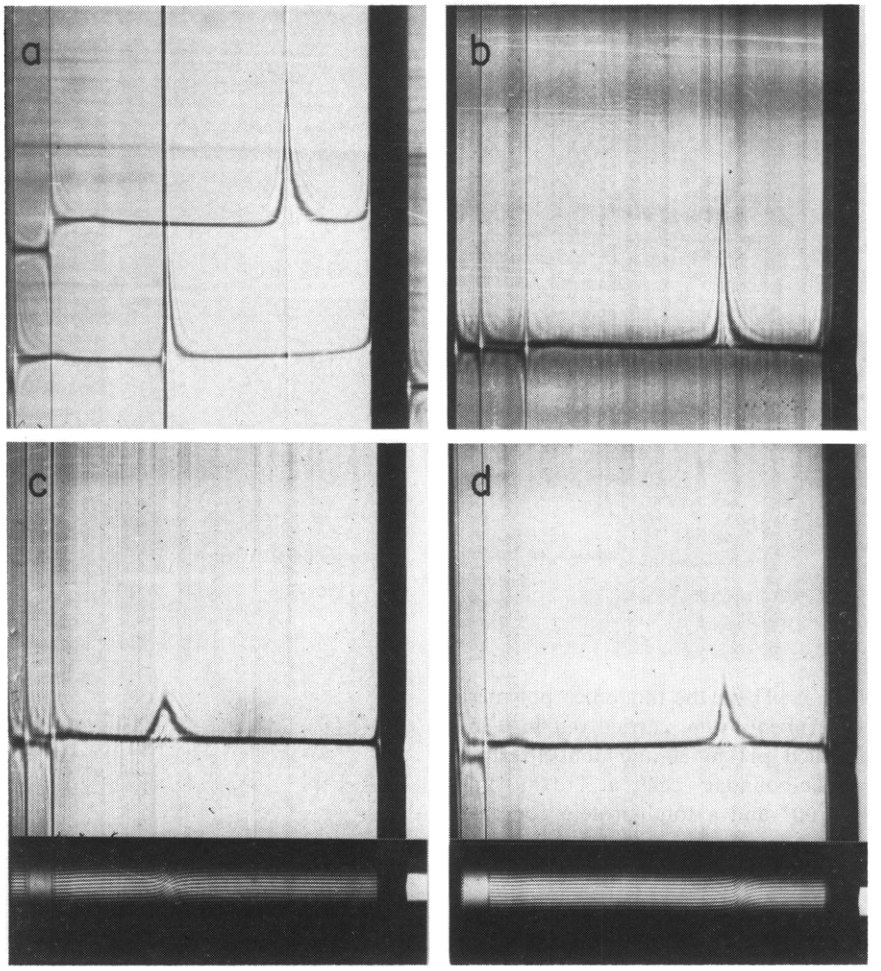

FIGURE 11: Sedimentation profiles of polymers formed by dialysis of monomeric myosin (in 0.5 M KCl) against pH 8.3, 0.137 M KCl buffer. Bar angle is 60°. (a) Protein concentration, regular cell 0.51%, wedge cell 0.29%; 25,980 rpm, 12-mm cell. (b) Protein concentration 0.21%, 19,610 rpm, 12-mm cell. (c) Protein concentration 0.05%, 13,410 rpm, 30-mm cell. (d) Protein concentration 0.16%, 21,740 rpm, 12-mm cell.

differential myosin monomer boundary (Schachman, 1959b) in that its sedimentation coefficient ($s_{20,w}$ = 4.4 S) is less than that of the original monomer boundary. This unusual sedimentation behavior appears to be the result of a shift in the monomer $\rightleftharpoons$ polymer equilibrium at high rotor velocity which favors the monomer species and emphasizes the delicate balance of the equilibrium state.[1]

Viscosity Studies. Polymer solutions used for viscosity studies were prepared by dialysis against pH 8.3, 0.137 M KCl solution (Materials and Methods). Each solution examined in the viscometer was also studied in the ultracentrifuge to provide a check on the reproducibility of the various samples. Monomer and polymer concentrations were determined from these runs by counting fringes across each boundary observed in the Rayleigh optical system.

Because of the high molecular weight and particle asymmetry of the 150S polymer the viscosity of the pH 8.3–0.137 M KCl system is markedly dependent on the shearing stress. The shear dependence is graphically illustrated in Figure 15 which presents reduced viscosity *vs.* shearing stress plots at constant protein concentration. The reduced viscosity at zero shearing stress obtained from Figure 15 is plotted against the polymer concentration in Figure 16 giving an intrinsic viscosity for the polymer of 2.07 dl/g.[2] In Figure 15 the curve for $c = 0$ describes the intrinsic viscosity as a function of the shearing stress, $[\eta]_\tau$ (Table II). Using the procedure described by Yang (1961) a rotary diffusion coefficient of 36–37 sec^{-1} was calculated. The length estimated from the rotary diffusion

[1] The formation of a differential boundary and the concomitant conversion of the polymer boundary to monomer are characteristically observed at pH 8.3, 0.17 M KCl. At lower salt concentrations (at pH 8.3), where the polymer is more strongly favored (and more stable) the perturbation of the equilibrium caused by increasing the rotor velocity does not result in loss of the integrity of the polymer boundary. This is probably because the destabilization of the polymer caused by increasing the rotor velocity is offset by the greater stability of the polymer at lower salt concentrations.

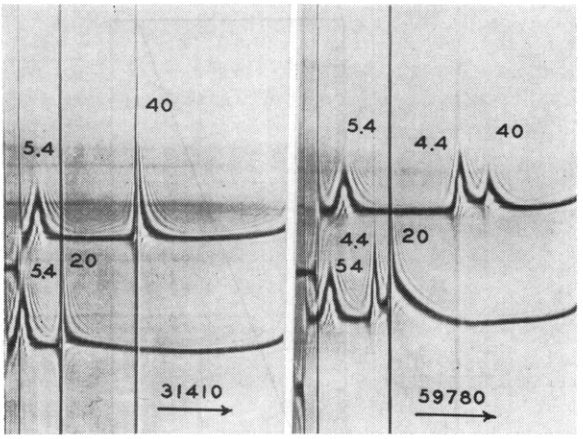

FIGURE 12: Effect of increasing rotor velocity on monomer–polymer equilibrium (pH 8.3, 0.17 M KCl). Protein concentration of lower pattern 0.66%, upper (wedge window) pattern 0.33%, 12-mm cell. Bar angle is 60°. The pattern on the right (59,780 rpm) was photographed 5 min after the pattern on the left (31,450 rpm).

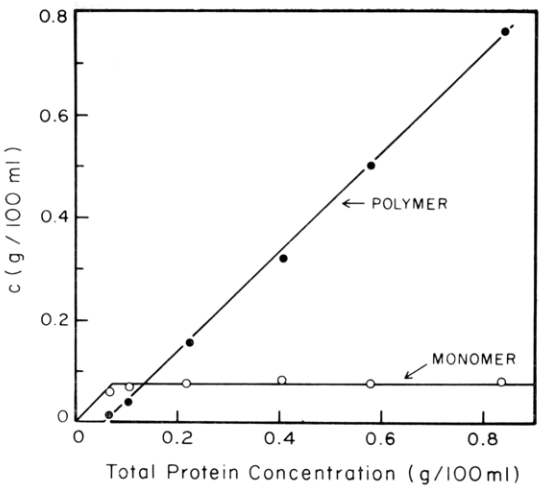

FIGURE 13: Plot of the monomer and polymer concentration against total (monomer + polymer) protein concentration. ——, calculated from eq 2 or Gilbert theory; (○), (●) experimentally observed values for 0.17 M KCl, pH 8.3.

TABLE II: Summary of Non-Newtonian Viscosity Data.

τ (dynes/cm^2)	3.0	2.39	1.73	0.51
$[\eta]_{cor}$ (dl/g)[a]	1.27	1.41	1.60	2.00
G (sec^{-1}) (5°)	198	158	114	33
$[\eta]_\tau/[\eta]_{\tau=0}$	0.61	0.68	0.77	0.97
α[c]	8.75	6.75	4.80	1.45
θ_w^{20} (sec^{-1})	36.0	37.2	37.8	36.2
L (A)[b] $= 2a$	6800	6700	6700	6800

[a] Corrected for inhomogeneous flow in the viscometer (Yang, 1961). [b] Calculated from Broersma (1960). $a^3 = \frac{3k}{8\pi}\left(\frac{T}{\theta\eta_0}\right)(\ln 2p - \gamma)$. $\gamma = 1.57 - 7\left(\frac{1}{\ln 2p} - 0.28\right)^2$. [c] Was obtained as a function of $[\eta]_\tau/[\eta]_{\tau=0}$ from Table XIII of Yang (1961).

coefficient using Perrin's (1934) equation and incorporating the modification suggested by Broersma (1960) (see also Haltner and Zimm, 1959) for rodlike particles is 6800 A.

In determining the intrinsic viscosity of the polymer it was necessary to make a correction for the small amount of monomer present in solution (0.10 mg/ml). As we have indicated above, and as we will discuss further below, the concentration of monomer remains constant over the protein concentration range spanned

[2] The data of Figure 16 has been utilized to obtain the Huggins (1942) constant (from the equation $\eta_{sp}/c = [\eta] + k[\eta]^2c$). An unusually high value of k ($k = 5.2$ g/dl) was obtained suggesting a large solvent–solute interaction. This would appear to be related to the sensitivity of the equilibrium system to salt concentration and pH.

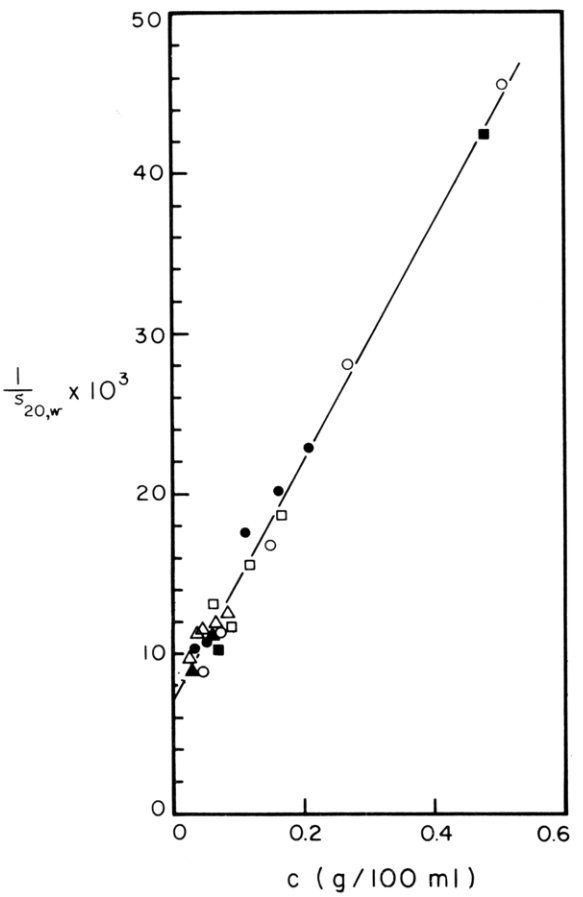

FIGURE 14: Reciprocal of the sedimentation coefficient ($1/s_{20,w}$) *vs.* concentration of myosin polymer formed at pH 8.3, 0.137 M KCl. The different symbols represent different polymer samples.

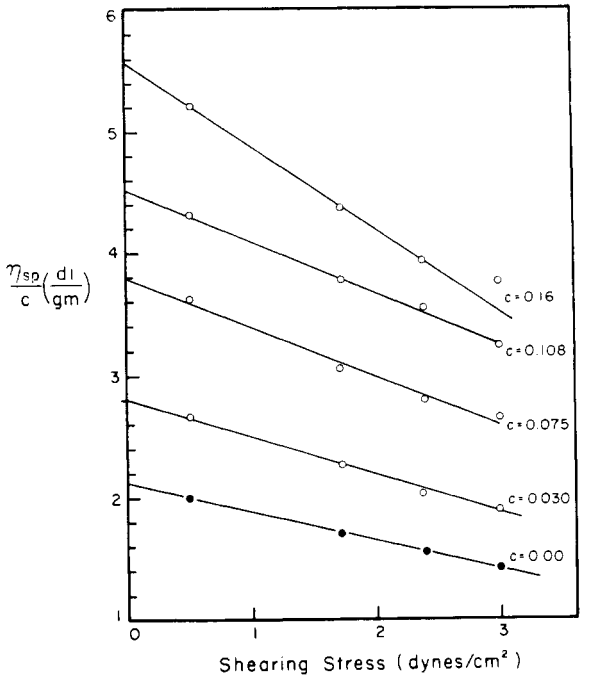

FIGURE 15: Reduced viscosity of solutions of myosin polymer formed at pH 8.3, 0.137 M KCl, as a function of shearing stress for different polymer concentrations (○).

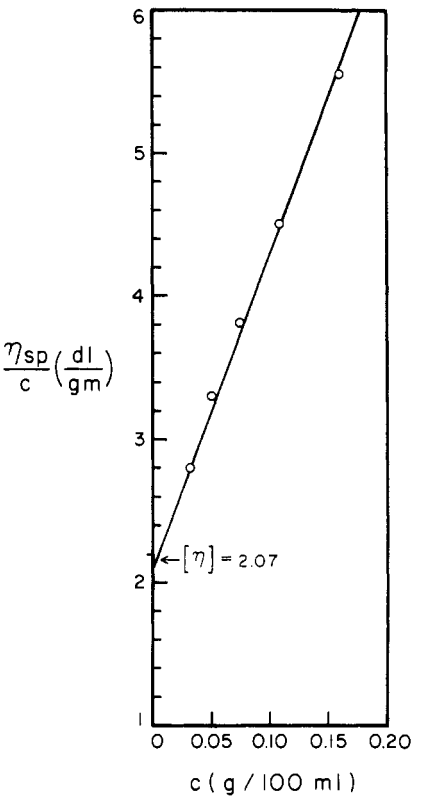

FIGURE 16: Reduced viscosity *vs.* concentration of myosin polymers (pH 8.3, 0.137 M KCl) at zero shearing stress.

in the viscosity studies. We assume that the specific viscosity of the solution is an additive function of the specific viscosities of monomer and polymer (Harrington and Schachman, 1953; Schachman, 1959a) and that only these two species are present in solution. (The narrow size distribution of the polymer particles seen in Figures 17 and 18 when taken in conjunction with the velocity sedimentation pattern of the pH 8.3, 0.137 M KCl polymer system provides evidence that there is no apparent tendency for the formation of a discrete particle intermediate in length between the 6300 A particle and the monomer.) Therefore, to obtain the viscosity of the polymer, the specific viscosity of the monomer ($[\eta]$ = 2.2 dl/g; Holtzer and Lowey, 1959) was subtracted from the measured specific viscosity of the solution.

Electron Microscope Studies of Myosin Polymers Formed at pH 8.3

Electron microscope studies of the pH 8.3, 0.137 M KCl myosin–polymer system show, consistent with the sedimentation patterns, a relatively sharp distribution of particle lengths (Figure 17). A length–distribution histogram of 178 particles is presented in Figure 18 indicating that about 70% of the particle lengths lie between 5600 and 7500 A with a mean length of all particles near 6300 A.

High magnification electron micrographs of the pH 8.3–0.137 M KCl system (Figure 17) reveal irregular surface corrugations along the polymer surface similar in gross appearance to those observed at low pH. A smooth central region is visible in the majority of particles. Although precise measurement of the average particle diameter is not possible because of the irregular surface projections, a reasonable estimate would be about 125 A. The smooth central region has a length in the range of 1800 A.

Discussion

The polymeric system formed at pH 8.3, 0.137 M KCl exhibits a single hypersharp boundary (150 S) in the ultracentrifuge and a relatively sharp size distribution in the electron microscope. The molecular properties of this polymer species have therefore been examined in detail.

Table III presents the molecular weight and particle dimensions of the 150S polymer estimated from both hydrodynamic and electron microscopic measurements. The relatively good agreement in the assembled molecular parameters derived from the various measurements summarized in Table III supports the view that they are a valid description of the particle as it actually exists in solution. It also supports the assumption that the high molecular weight particles seen in the electron micrographs are representative of the particle (150 S) whose properties are being measured in solution.

In earlier sections of this paper evidence pertaining to the equilibrium nature of the monomer–polymer

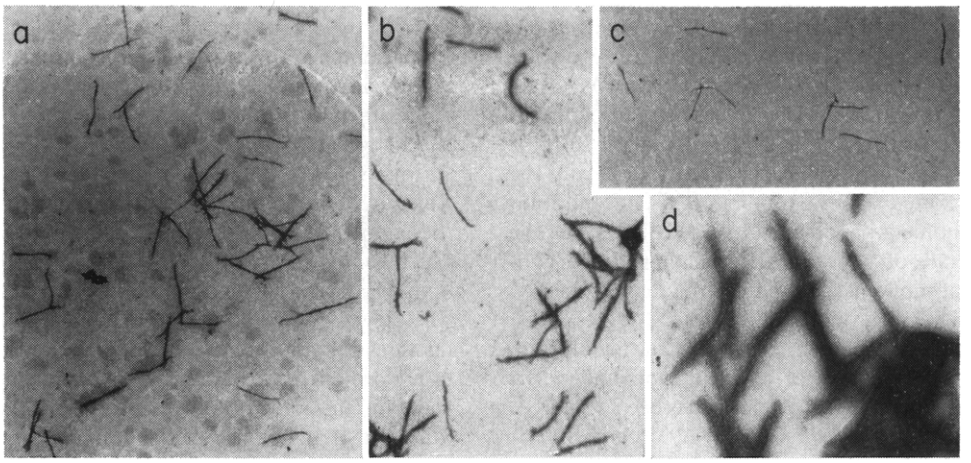

FIGURE 17: Myosin polymers formed by dialysis of monomeric myosin (in 0.5 M KCl) against pH 8.3, 0.137 M KCl. See Figure 18 for length distribution. The polystyrene spheres are 1880 A in diameter.

TABLE III: Physical Parameters of Myosin Polymers Formed at pH 8.3, 0.137 M KCl.

$s^0_{20,w}$ = 150 S	$M_w = 52 \times 10^6$ g/mole[d]
$[\eta]$ = 2.07 dl/g	$M_w = 47 \times 10^6$ g/mole[e]
$\theta^{20}_w = 36.5$ sec^{-1}	Diameter = 120 A[f]
Length = 6300 A[a]	Diameter = 100–130 A[a]
Length = 7600 A[b]	Axial ratio = 62[g]
Length = 6800 A[c]	Axial ratio = 52[h]

[a] Estimated from electron micrographs (see Figures 17 and 18). [b] Estimated from $[\eta]$ and M_w (Yang, 1961). [c] Estimated from rotary diffusion coefficient (see Table II and Broersma, 1960). [d] Estimated from $[\eta]$ and $s^0_{20,w}$ (Scheraga and Mandelkern, 1953). Recently it has been suggested (Holtzer and Lowey, 1963) that the β values customarily used in conjunction with the Scheraga–Mandelkern equation may not be appropriate for rodlike particles. Using the theory of Kirkwood *et al.* (1950, 1951), which approximates a rigid rod as a rigid string of identical spherical beads, Holtzer and Lowey have calculated β values for rodlike particles. If the β values thus calculated are used, then molecular weights determined from the modified form of the Scheraga–Mandelkern equation are about 20% higher than those calculated from the β values originally proposed by Scheraga and Mandelkern (1953). [e] Estimated from $[\eta]$ and θ^{20}_w (Scheraga and Mandelkern, 1953). [f] Estimated from $s^0_{20,w}$ (Peacocke and Schachman, 1954). [g] Estimated from $[\eta]$ (Simha, 1940). [h] Estimated from length determined by electron microscopy and diameter determined from $s^0_{20,w}$.

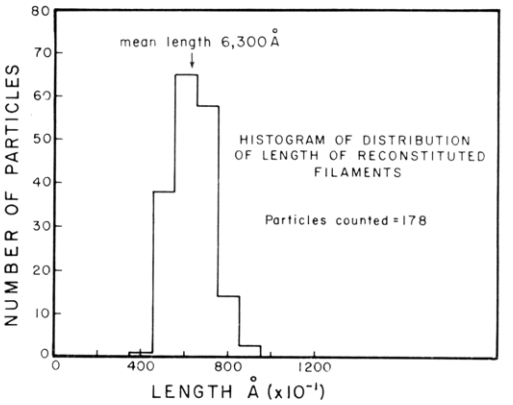

FIGURE 18: Histogram of distribution of lengths of myosin polymers formed at pH 8.3, 0.137 M KCl; 178 particles counted.

system has been presented. Consider the simple case of a monomer in equilibrium with a high molecular weight polymer where only the two species monomer and n-mer are present in detectable concentrations. We may then write

$$n \text{ monomer} \rightleftarrows \text{polymer} \qquad (1)$$

and

$$K = \frac{[\text{polymer}]}{[\text{monomer}]^n} = \frac{[P]}{[M]^n} \qquad (2)$$

and $\log K = \log [P] - n \log [M]$, where [P] is the molar concentration of polymer, [M] the molar concentration of monomer, and n the number of monomer units in the polymer. At pH 8.3, 0.17 M KCl where $n = (50 \times 10^6)/(6 \times 10^5) = 83$, it was observed experimentally that the concentration of monomer in a velocity sedimentation pattern was 0.076% and the polymer concentration was 0.097% from area measurements of the respective sedimenting boundaries. Then the approximate value of the equilibrium constant is $K = 10^{482}$ at 5°.[3] In this calculation the molar concentration of monomer was based on a molecular weight of 6

[3] It should be understood that the equilibrium constant thus calculated is the "average" equilibrium constant for formation of the polymer. We do not wish to imply that the free energy per monomer incorporated, $\Delta F = -(RT/n) \ln K$, is the same for every monomeric unit. That this cannot be the case is clear since the polymer particles grow to a specific size.

$\times 10^5$ [4] (Kielley and Harrington, 1960; Woods *et al.*, 1963), and the molar concentration of the polymer was based on a molecular weight of 50×10^6. Using the value of K above we have calculated the concentration of monomer to be expected for the 0.17 M KCl system at various polymer concentrations and the results are plotted against total protein concentration (sum of monomer + polymer) in Figure 13. Over the complete range of concentrations examined the concentrations of monomer and polymer actually observed show good agreement with the theoretical values based on the simple monomer $\rightleftharpoons$ polymer equilibrium formulation. Two ranges of concentration under two sets of ionic conditions at pH 8.3 have been explored. In both systems (0.137 M KCl, $K = 10^{550}$ and 0.17 M KCl, $K = 10^{482}$) the monomer concentration remains constant at a value determined by the ionic conditions. The constancy of the monomer concentration follows directly from the equilibrium formulation, given the high value of n, the number of units in the polymer. As the total protein concentration decreases, the monomer concentration remains constant, at a value characteristic of the prevailing salt and pH conditions, while there is a continual drop in the polymer concentration. Only after the polymer concentration approaches zero does the monomer concentration begin to decrease, as can be seen in Figure 13. For example, at a monomer concentration of 0.074% the polymer concentration at equilibrium is 0.01%, whereas at a monomer concentration of 0.070% the polymer concentration is 1.15×10^{-4}%, *i.e.*, a decrease of approximately 100-fold. This behavior is analogous to that commonly observed for micelles containing large numbers of monomer units in that the concentration of monomer remains nearly constant as the total concentration is varied.

These unusual features of the pH 8.3 monomer–polymer system have interesting implications in the interpretation of sedimentation velocity patterns. Since the monomer concentration remains constant within experimental error over a wide range of polymer concentration, there is a negligibly small change of monomer concentration across the polymer boundary. It appears that this is the reason that the area of the polymer boundary (corrected for radial dilution) in a transport experiment is a very close approximation of the concentration of this species present in the initial solution. In the region between the two boundaries, although a concentration gradient must be present, its magnitude is so low as to be virtually undetectable over the concentration range employed in our experiments. Thus within the limits of the schlieren optical system the monomer and polymer boundaries appear to be completely resolved and measurement of the fringe count or the areas of the individual peaks give a good estimate of their true concentration in solution.

Gilbert (1955, 1958, 1959) has developed a detailed theory for a monomer $\rightleftharpoons$ polymer system in which the rate of attainment of equilibrium is rapid,[5] and has considered the shapes of the species boundaries. Such systems, in general, show partial resolution of two boundaries with the sedimentation coefficient of the slower sedimenting boundary remaining constant, as does the area under this boundary with decreasing total protein concentration. The sedimentation coefficient of the more rapidly sedimenting boundary goes through a maximum with decreasing concentration and the area of the boundary decreases. The two boundaries observed cannot be identified in terms of specific species since all volume elements in the cell are in monomer $\rightleftharpoons$ polymer equilibrium. Many of these features such as partial resolution of the two peaks (that is, an elevation of the base line between the two boundaries), the variation in sedimentation coefficient with concentration of the more rapidly sedimenting boundary, and the lack of identity of a particular boundary with a given species in solution can be attributed to the existence of both monomer and polymer concentration gradients between the two boundaries. Calculations of monomer and polymer concentration gradients using Gilbert theory for the myosin $\rightleftharpoons$ polymer system described above show that although such gradients exist, their magnitude is exceedingly small. This results in (1) an apparently flat base line and complete resolution between monomer and polymer boundaries, (2) the boundaries observed correspond to the two species present to a good approximation, and (3) the sedimentation coefficient of the polymer boundary shows normal s *vs.* c behavior rather than the inversion predicted from the Gilbert theory. All of these consequences are a result of the large number of monomeric units in the polymer species, the absence of intermediates in this system, and an equilibrium constant strongly favoring the formation of the polymeric species.

We have already discussed the sensitivity of the myosin $\rightleftharpoons$ polymer equilibrium system to small variations in ionic strength (Figure 10). The sedimentation pattern presented in Figure 12 demonstrates that the equilibrium is also very sensitive to the rotor velocity during ultracentrifugation. At low speed (*ca.* 13,000 rpm) and at concentrations below 0.15%, the double-sector cell experiments showed no elevation in the base line between monomer and polymer boundary,

[4] Using a molecular weight of 5×10^5 (see Gergely, 1966; Kielley, 1964; Tonomura *et al.*, 1966; and Holtzer and Lowey, 1959, for a discussion of the different estimates of the molecular weight of myosin) will increase the value of n to 100, and correspondingly change the calculated equilibrium constant. However the properties of the monomer–polymer equilibrium being considered here are insensitive to the actual number of monomeric units in the polymer so long as the number is large.

[5] An attempt was made to measure the rate of formation of the myosin polymers by following the increase of scattered (90°) light after mixing equal volumes of distilled water and monomer in 0.274 M KCl buffer. It was found that, within the brief period required for mixing the water and monomer solutions and placing them in the light-scattering photometer (*ca.* 45 sec), the measured scattering had already reached the value observed for polymer solutions of the same protein concentration.

and the fringe pattern displayed in the Rayleigh optical system was straight in this region (Figure 11). When experiments were performed at speeds of the order of 33,000 rpm the base line was elevated slightly, and the fringe pattern in the interference optical system showed a positive slope throughout the cell. At high speed (59,780 rpm) the schlieren base line between monomer and polymer is markedly elevated and the polymer boundary is continuously depleted as it moves through the cell. The explanation for this behavior appears to be that the polymer is continuously dissociating into monomer as it moves through the centrifuge cell under these conditions as shown by the experiment illustrated in Figure 12. The fundamental reasons for this phenomenon are not clear at the present time. We are investigating the possibility that the shift in the equilibrium at high rotor velocity stems from the hydrostatic pressure gradient in the centrifuge cell, suggesting a difference in the partial specific volumes of the monomer and polymer species.[6]

Particles formed in the pH 6.2–7.3 (type III) and the pH 8–8.5 myosin systems exhibit features (Figures 7 and 17) common to the native thick filaments of the myofibril reported by Huxley (1960, 1963). It seems likely, therefore, that both of the high molecular weight synthetic polymers (180 and 150 S) described in this paper and the native thick filament may have a common structural pattern. The fact that we can obtain a very sharp length distribution for the 6500 A particle (150 S) and that the length of the basic structure can be varied by varying the salt and pH suggests that the specific ionic environment in the developing muscle cell may determine the cut-off length of the native thick filament. In the present study we have examined the effect of varying the KCl concentration and pH on the polymerization process. It seems possible that the type of ion in the ionic environment or the temperature may well be crucial in establishing the length of the thick filament. Although it appears that polymer particles of a specific length and structure can be determined exclusively by the ionic environment, we cannot rule out the existence of a central core material whose function would be to establish the length of the native thick filament in a manner analogous to the ribonucleic acid of tobacco mosaic virus.

Acknowledgment

The authors with to thank Dr. C. A. Thomas for the loan of the three-bulb viscometer. We are indebted to Shirley Varricchio for invaluable assistance in the preparation of this manuscript.

[6] We have recently obtained further information supporting the view that the effects related to high rotor velocity result from dissociation of the polymer and are caused by the hydrostatic pressure gradient. In these experiments the hydrostatic pressure was varied by layering a nonmiscible liquid over the myosin solution. Under these conditions the concentration of polymer in the equilibrium system was found to decrease with increasing pressure head (R. Josephs and W. F. Harrington, in preparation, 1966; Josephs, 1966).

References

Broersma, S. (1960), *J. Chem. Phys., 32*, 1626.
Gergely, J. (1966), *Ann. Rev. Biochem. 35*, 691.
Gilbert, G. A. (1955), *Discussions Faraday Soc. 20*, 68.
Gilbert, G. A. (1958), *Discussions Faraday Soc. 25*, 224.
Gilbert, G. A. (1959), *Proc. Roy. Soc. (London), A250*, 377.
Gilbert, G. A., and Gilbert, L. M. (1962), *Nature 194*, 1173.
Haltner, A. J., and Zimm, B. H. (1959), *Nature 184*, 265.
Harrington, W. F., and Schachman, H. K. (1953), *J. Am. Chem. Soc. 75*, 3533.
Holtzer, A., and Lowey, S. (1959), *J. Am. Chem. Soc. 81*, 1370.
Holtzer, A., and Lowey, S. (1963), *Biopolymers 1*, 497.
Huggins, M. L. (1942), *J. Am. Chem. Soc. 64*, 2716.
Huxley, H. E. (1960), *in* The Cell, Vol. IV, Brachet, J., and Mirsky, A. E., Ed., New York, N. Y., Academic, p 365.
Huxley, H. E. (1963), *J. Mol. Biol. 7*, 281.
Jakus, M. A., and Hall, C. E. (1947), *J. Biol. Chem. 167*, 705.
Josephs, R. (1966), Ph.D. Dissertation, Johns Hopkins University, Baltimore, Md.
Kaminer, B., and Bell, A. L. (1966), *Science 152*, 323.
Kielley, W. W. (1964), *Ann. Rev. Biochem. 33*, 403.
Kielley, W. W., and Bradley, L. B. (1956), *J. Biol. Chem. 218*, 653.
Kielley, W. W., and Harrington, W. F. (1960), *Biochim. Biophys. Acta 41*, 401.
Kirkwood, J. G., and Auer, P. (1951), *J. Chem. Phys. 19*, 281.
Kirkwood, J. G., and Riseman, J. (1950), *J. Chem. Phys. 18*, 512.
Nichol, L. W., Bethune, J. L., Kegeles, G., and Hess, E. L. (1964), *Proteins 2*, 305.
Noda, H., and Ebashi, S. (1960), *Biochim. Biophys. Acta 41*, 386.
Peacocke, A. R., Schachman, H. K. (1954), *Biochim. Biophys. Acta 15*, 198.
Perrin, F. (1934), *J. Phys. Radium* [7] *5*, 497.
Schachman, H. K. (1959a), *in* Ultracentrifugation in Biochemistry, New York, N. Y., Academic, p 90.
Schachman, H. K. (1959b), *in* Ultracentrifugation in Biochemistry, New York, N. Y., Academic, p 103.
Scheraga, H. A., and Mandelkern, L. (1953), *J. Am. Chem. Soc. 75*, 179.
Simha, R. (1940), *J. Phys. Chem. 44*, 25.
Tonomura, Y., Appel, P., and Morales, M. (1966), *Biochemistry 5*, 515.
Woods, E. F., Himmelfarb, S., and Harrington, W. F. (1963), *J. Biol. Chem. 238*, 2374.
Yang, J. T. (1961), *Advan. Protein Chem. 16*, 323.
Zobel, C. R., and Carlson, F. D. (1963), *J. Mol. Biol. 7*, 78.